Supplementary Information

Dual-Targeting Macrophage Membrane Nanosystem Enhances Radiotherapy-Induced Antitumor Immunity via Synergistic Nuclear and Mitochondrial DNA Damage

Guangyu Ju, [†a,c] *Qi Ding,* [†c] *Hongcang Gu,* [†c] *Rao Liu,*[a,c] *Xiao Liu,*[c] *Zimeng Wang,*[c] *Kaiwei Wang,*[c] *Yuan Ping,*[*d] *Jian You,*[*d] *Shuanghu Yuan,*[*a,b] *and Junchao Qian*[*a,b,c]

a. Department of Radiation Oncology, The First Affiliated Hospital of USTC, Division of Life Sciences and Medicine, University of Science and Technology of China, Hefei, Anhui, 230031, P.R. China.

b. Department of Radiation Oncology, Anhui Provincial Cancer Hospital, Hefei, Anhui, 230031, P.R. China.

c. Anhui Province Key Laboratory of Medical Physics and Technology, Institute of Health and Medical Technology, Hefei Institutes of Physical Science, Chinese Academy of Sciences, Hefei 230031, P.R. China.

d. College of Pharmaceutical Sciences, Zhejiang University, 866 Yuhangtang Road, Hangzhou, Zhejiang, 310058, P. R. China.

*Correspondence to: Junchao Qian (qianjunchao@ustc.edu.cn), Yuanshuang Hu (yuanshuanghu@sina.com), Jian You (youjiandoc@zju.edu.cn), or Ping Ying (pingy@zju.edu.cn)

† These authors contributed equally to this work.

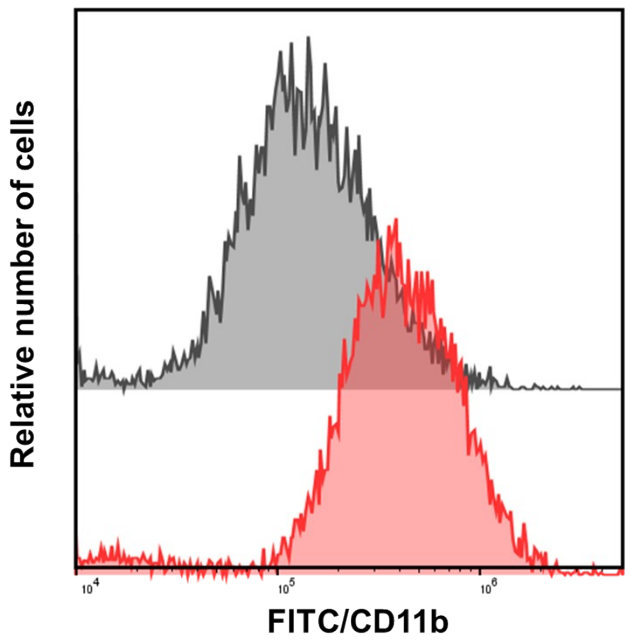

Fig. S1. Flow cytometry analysis of CD11b expression on macrophage membranes. Macrophages were incubated with conditioned medium derived from tumor cells exposed to low-dose (2 Gy) irradiation. Flow cytometry revealed a significant upregulation of CD11b on macrophage membranes compared to control groups. This increase reflects activation of innate immune signaling pathways triggered by damage-associated molecular patterns (DAMPs) such as mitochondrial DNA and HMGB1 released from irradiated tumor cells, thereby enhancing macrophage adhesion capabilities critical for tumor targeting and blood–brain barrier penetration.

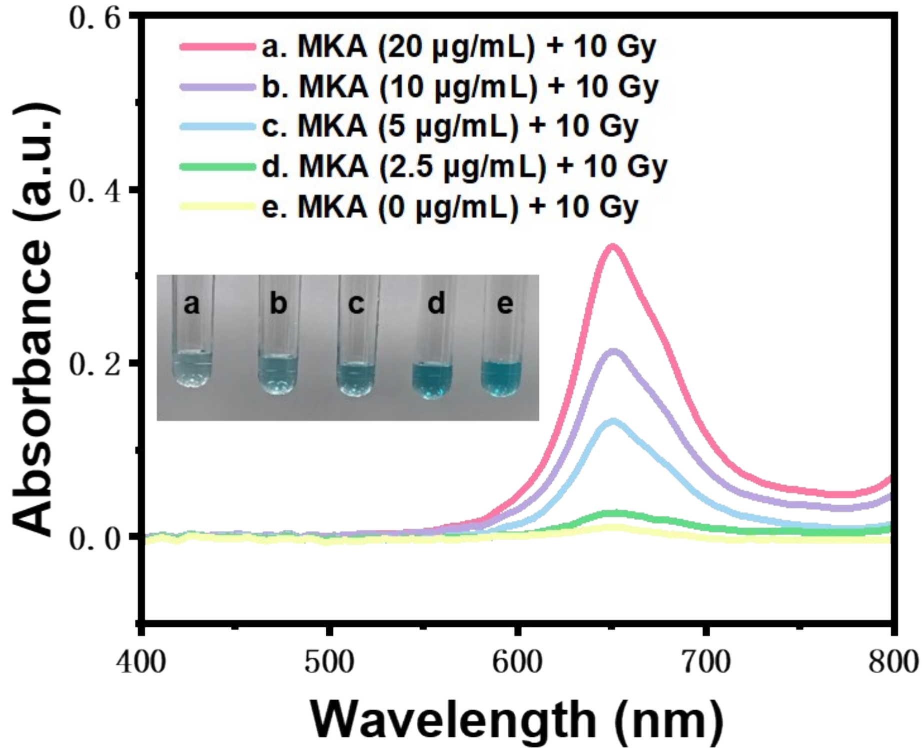

Fig. S2. X-ray-induced hydroxyl radical (•OH) generation by MKA in a dose-dependent manner. Photographic and corresponding UV–Vis spectrophotometric analysis of TMB oxidation upon treatment with increasing concentrations of MKA (0, 2.5, 5, 10, and 20 μg/mL) under 10 Gy X-ray irradiation. Enhanced blue coloration and elevated absorbance at 652 nm indicate dose-dependent •OH production via Fenton-like activity of MKA under radiative conditions.

Gene	Mean fold change (2^-ΔΔCt)	SD	log2(Mean)	P-value
12S	239.34	421.93	7.90	<0.01（0.0061）
COX1	1749.33	2982.11	10.77	<0.001（1.66×10^{-5}）
D-loop	127.93	221.46	7.00	<0.001（5.25×10^{-5}）
N-A	197.63	472.82	7.63	<0.05（0.0433）
ND1	169.67	152.18	7.41	<0.001（0.00089）

Table. S1. Fold changes were calculated using the 2^-ΔΔCt method. Data are presented as mean ± SD (n = 6). Statistical significance was determined using an unpaired two-tailed t-test based on ΔCt values.

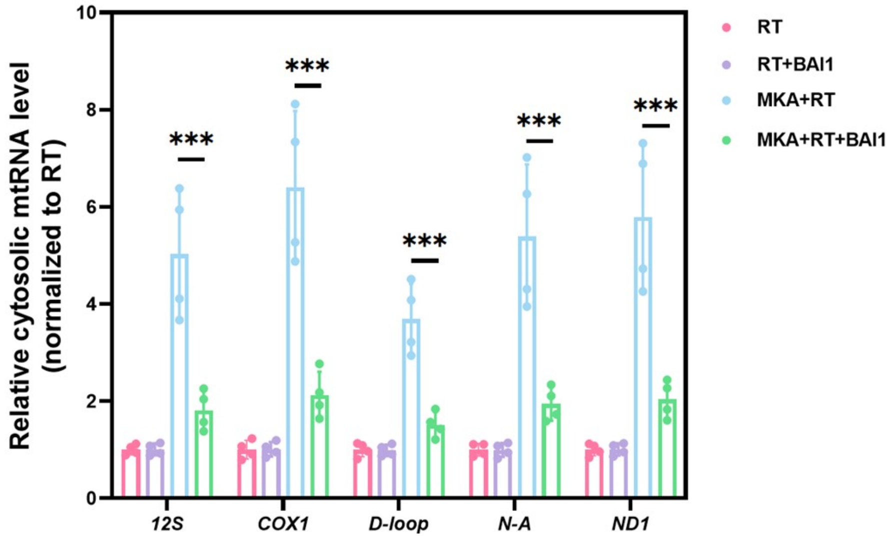

Fig. S3. BAX inhibition reduces cytosolic mtRNA accumulation induced by MKA+RT. RT-qPCR analysis of cytosolic mitochondrial RNA species (12S, COX1, D-loop, N-A, and ND1) in cells treated with RT, RT+BAI1, MKA+RT, or MKA+RT+BAI1. Data were normalized to the RT group and are presented as mean ± SD (n = 6). Statistical significance was analyzed using two-way ANOVA with Dunnett's multiple comparisons test. ***$P < 0.001$.

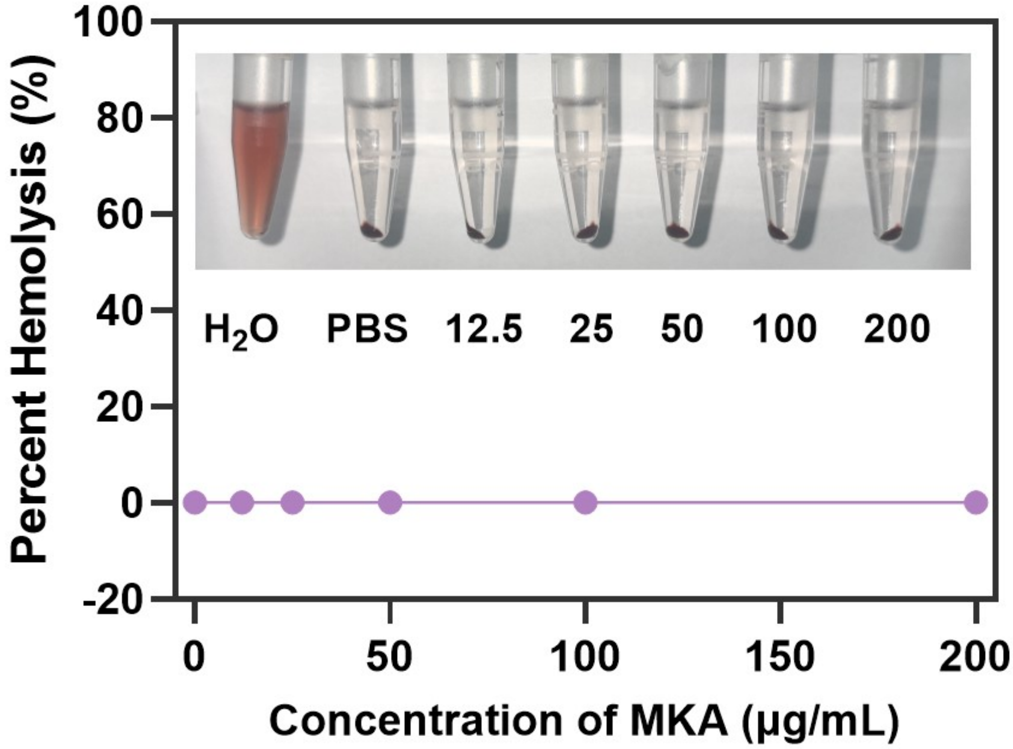

Fig. S4. Hemolysis assay of MKA at various concentrations. Photographs of red blood cell suspensions incubated with MKA at concentrations of 200, 100, 50, 25, and 12.5 μg/mL, along with PBS (negative control) and deionized water (positive control), accompanied by the corresponding hemolysis percentage displayed as bar graphs within the same figure. Results demonstrate negligible hemolytic activity of MKA at all tested concentrations. Data represent mean ± SD (n = 3).

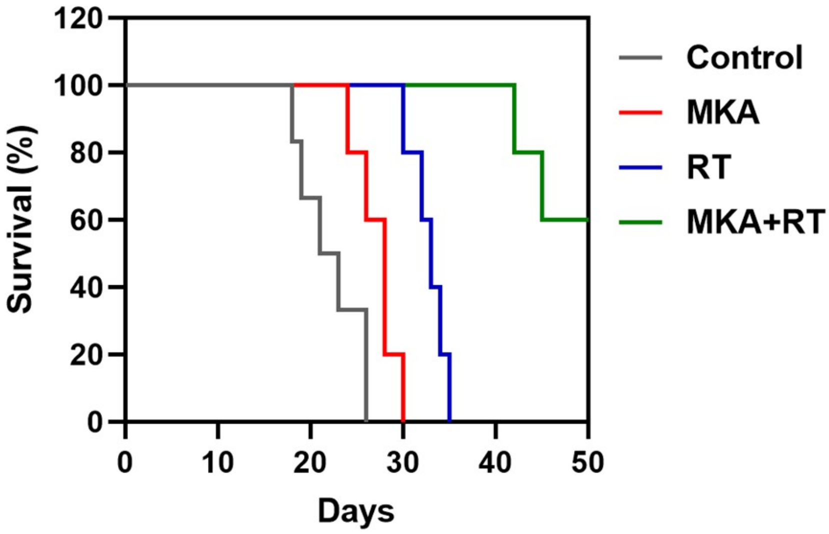

Fig. S5. Kaplan–Meier survival analysis of mice bearing orthotopic GL261 gliomas after different treatments. Kaplan–Meier survival curves of tumour-bearing mice in the Control, MKA, RT, and MKA+RT groups (n = 5). Mice treated with the combined MKA+RT regimen showed the longest survival compared with the other groups, indicating an improved therapeutic benefit in the orthotopic glioma model.

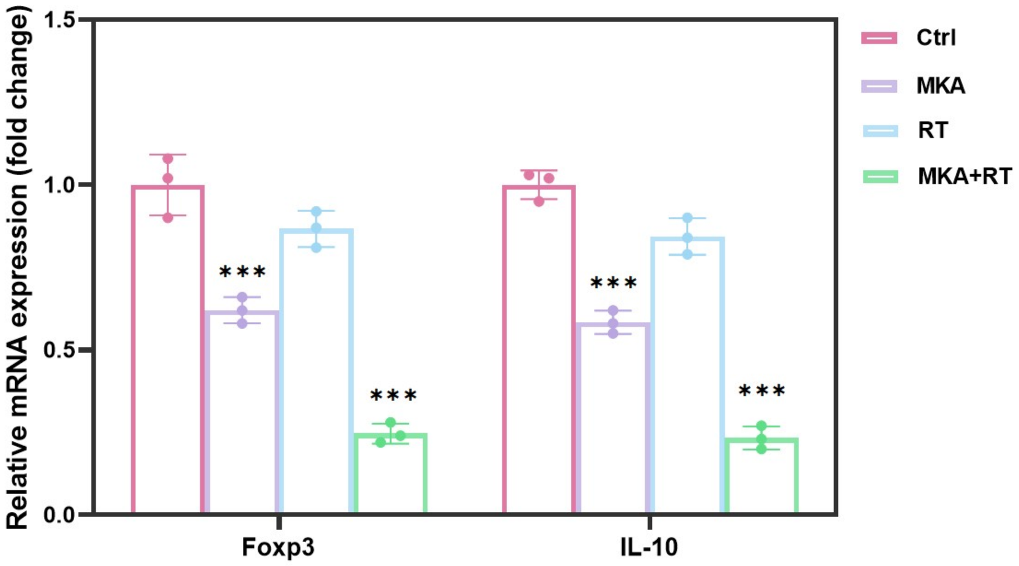

Fig. S6. qPCR analysis of Foxp3 and IL-10 expression in GL261 tumors after different treatments. Expression levels were normalized to GAPDH and presented as fold change relative to control. Combination treatment (MKA+RT) significantly reduced Foxp3 and IL-10 expression, indicating decreased Treg-associated immunosuppression. Data represent mean ± SD (n = 3). statistical significance determined by two-way ANOVA with Tukey's post hoc test. $^{*}P < 0.05$; $^{**}P < 0.01$; $^{***}P < 0.001$.

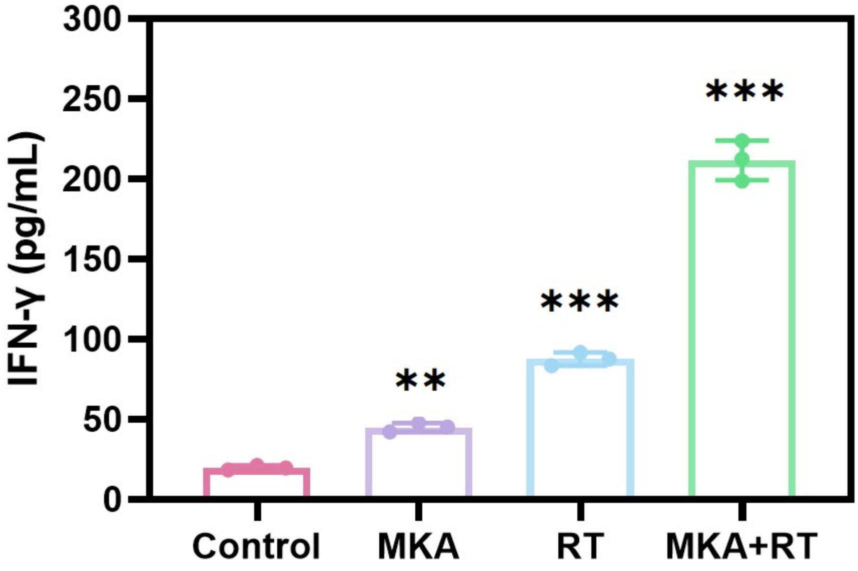

Fig. S7. IFN-γ secretion by splenocytes isolated 45 days after treatment and restimulated ex vivo with GL261 tumor antigens. MKA+RT markedly increased antigen-induced IFN-γ release, indicating enhanced long-term functional immune memory. Data represent mean ± SD (n = 3). one-way ANOVA with Tukey correction. $^{*}P < 0.05$; $^{**}P < 0.01$; $^{***}P < 0.001$.

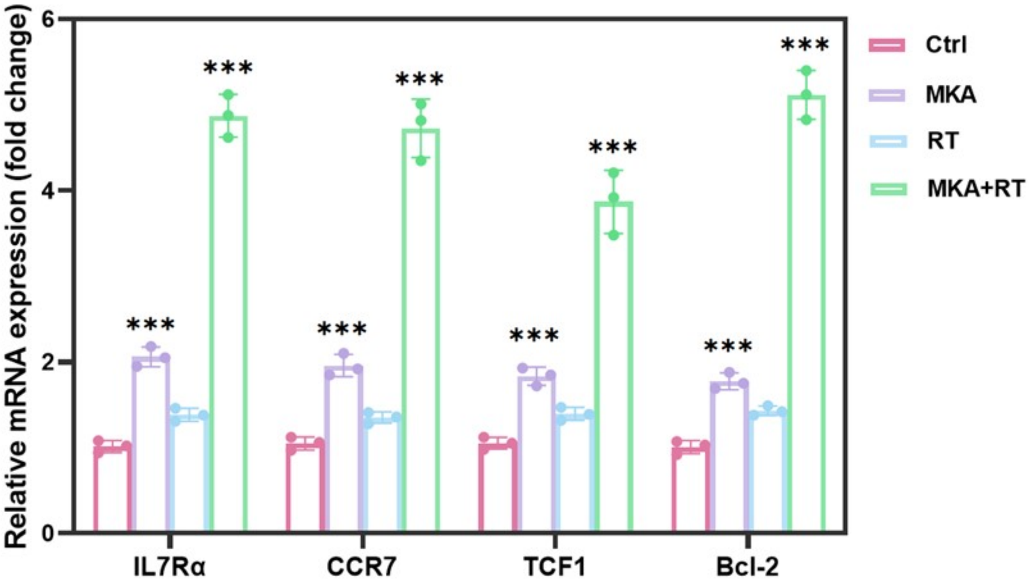

Fig. S8. qPCR quantification of memory-associated genes (IL7Rα, CCR7, TCF1, Bcl-2) in splenocytes 45 days after treatment. Expression levels were normalized to GAPDH and shown as fold change relative to control. MKA+RT significantly upregulated multiple memory-programming genes. Data represent mean ± SD (n = 3). two-way ANOVA with Tukey's post-test. $^{*}P < 0.05$; $^{**}P < 0.01$; $^{***}P < 0.001$.

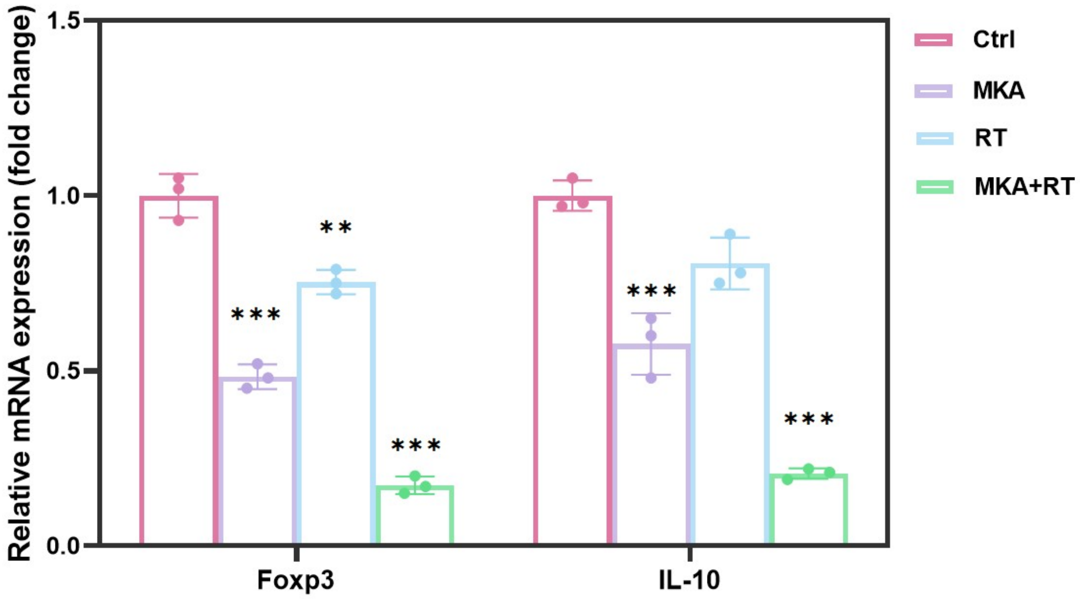

Fig. S9. qPCR analysis of Foxp3 and IL-10 expression in 4T1 tumors following treatment. Expression was normalized to GAPDH and presented as fold change relative to control. MKA+RT reduced Treg-related gene expression, consistent with alleviated intratumoral immunosuppression. Data represent mean ± SD (n = 3). two-way ANOVA with Tukey's post-test. $^{*}P < 0.05$; $^{**}P < 0.01$; $^{***}P < 0.001$.

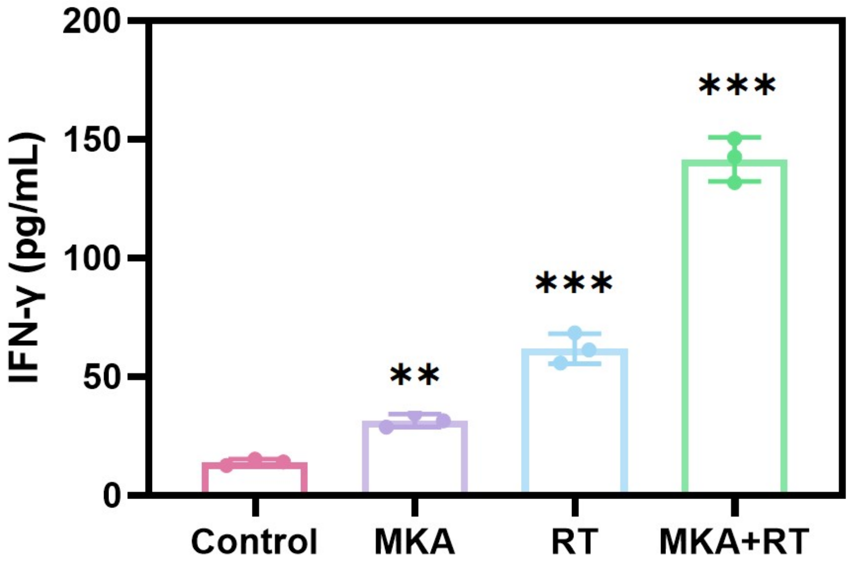

Fig. S10. IFN-γ release from splenocytes isolated 45 days after treatment and restimulated with 4T1 tumor antigens. The MKA+RT group showed the highest IFN-γ production, demonstrating durable systemic immune memory. Data represent mean ± SD (n = 3). one-way ANOVA with Tukey's post-test. $^{*}P < 0.05$; $^{**}P < 0.01$; $^{***}P < 0.001$.

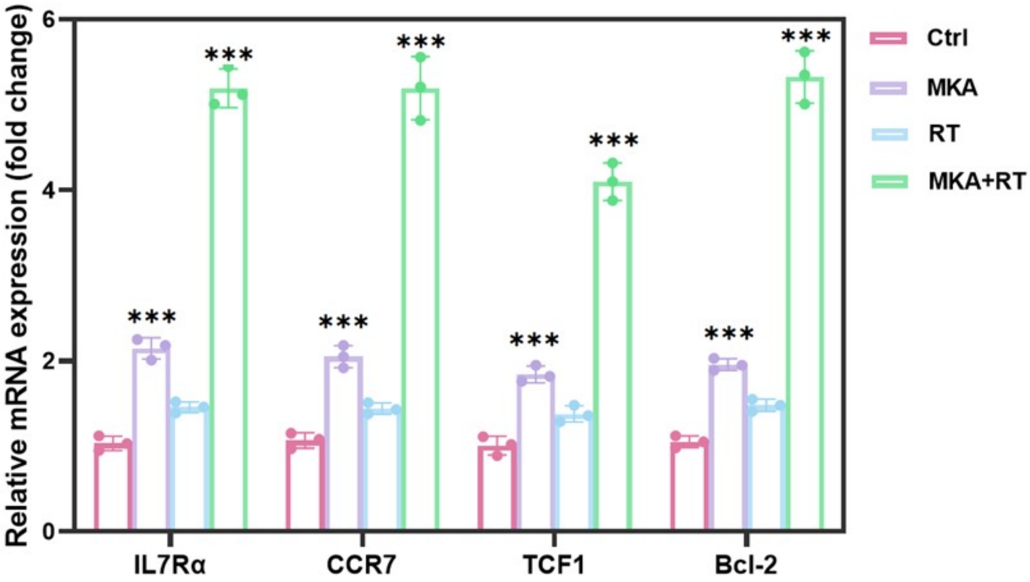

Fig. S11. qPCR expression of IL7Rα, CCR7, TCF1, and Bcl-2 in splenocytes collected 45 days after treatment. Data were normalized to GAPDH and expressed as fold change relative to control. MKA+RT significantly enhanced memory-associated transcriptional programming. Data represent mean ± SD (n = 3). two-way ANOVA with Tukey's post-test. $^{*}P < 0.05$; $^{**}P < 0.01$; $^{***}P < 0.001$.